Dyes and Pigments 81 (2009) 174–179

Contents lists available at ScienceDirect

Dyes and Pigments

journal homepage: www.elsevier.com/locate/dyepig

Blue light-emitting diodes from 2-(10-naphthylanthracene)-spiro[fluorene-7,9′-benzofluorene] host material

Kyu-Sung Kim [a], Hyun Seok Lee [a], Young-Min Jeon [a], Joon-Woo Kim [b], Chil-Won Lee [b], Myoung-Seon Gong [a,*]

[a] Department of Chemistry and Institute of Basic Sciences, Dankook University, Chungnam 330-714, South Korea
[b] OLED Team, Daejoo Electronic Materials, Siheung, Kyung-gi 429-848, South Korea

ARTICLE INFO

Article history:
Received 13 June 2008
Received in revised form
7 September 2008
Accepted 8 September 2008
Available online 17 October 2008

Keywords:
Blue OLED
Host
Dopant
Spiro[fluorene-benzofluorene]
Color purity
Spiro compound

ABSTRACT

A novel, spiro-type host material 2-(10-naphthylanthracene)-spiro[fluorene-7,9′-benzofluorene] was prepared by reacting 2-bromo-spiro[fluorene-7,9′-benzofluorene] with 9-(2-naphthylanthracene)-10-boronic acid via the Suzuki reaction. 2-4′-(Phenyl-4-vinylbenzeneamine)phenyl-spiro[fluorene-7,9′-benzofluorene], 4-[2-naphthyl-4′(phenyl-4-vinylbenzeneamine)]phenyl and diphenyl-[4-(2-[1,1;4,1]terphenyl-4-yl-vinyl)-phenyl]-amine were used as dopant materials. Devices with the configuration of ITO/*N*,*N*′-bis[4-(di-*m*-tolylamino)phenyl]-*N*,*N*′-diphenylbiphenyl-4,4′-diamine)/bis[*N*-(1-naphthyl)-*N*-phenyl]benzidine/2-(10-naphthylanthracene)-spiro[fluorene-7,9-benzofluorene]:5% dopant/aluminum tris(8-hydroxyquinoline)/Al-LiF showed a maximum power efficiency of 3.7 cd/A at 17.93 mA/cm^2 and a maximum luminance of 5018 cd/m^2 at 10 V with a turn-on voltage of 4.5 V.

1. Introduction

Organic π-conjugated materials continue to attract considerable interest because of their potential applications in various optoelectronic devices, especially in organic light-emitting diodes (OLEDs) [1]. Much of the recent research into blue-emitting materials has centered on styryl-based derivatives because of their high solution and solid-state photoluminescence quantum yields [2–4]. Recently, anthracene derivatives have been considered as suitable candidates for producing highly efficient and stable blue light emission [5,6]. Since Tour and coworkers introduced the spirobifluorene unit into organic electronics in 1996, spirobifluorene-containing oligomers and polymers have become promising candidates for electroluminescent materials due to their high luminescence efficiency, good carrier mobility and excellent thermal stability [7–9]. Salbeck et al. exploited spirobifluorene building blocks to construct various oligomers [10]. Fully spiro-configured terfluorenes, spirobifluorene trimmers and spirobifluorene linked with anthracene and aryl amine moiety have also been synthesized and used as blue light-emitting materials with high thermal stability [8,9,11]. Carrier-transporting materials based on spirobifluorene with a high T_g temperature show excellent non-dispersive hole-transporting and ambipolar carrier-transporting properties [12]. However, the disadvantage of these types of oligomers is the difficulty of tuning the electronic structure and incorporating other functional groups, which greatly limits their applications in the field of organic electronics and the construction of complicated optoelectronic systems. Incorporating aromatic substituents would be a useful method of expanding the application of spiro compounds. However, spiro compounds with versatile substituents, especially spirobifluorene with an asymmetric substitution of the fluorene units, have seldom been reported [13–18]. To explore this complicated light-emitting system and gain a better insight into the effect of the substitution on the electronic structure, we successfully prepared the host and dopant materials based on spiro[fluorene-benzofluorene]. There are three possible positions (2, 9 and 2′) in the spiro[fluorene-benzofluorene] molecule. Connecting anthracene chromophore by the above spiro linkage can result in quite unexpected optical properties if there is an electronic interaction via the spiro carbon atom. The introduction of aromatic substitution at the 2-position of spiro[fluorene-benzofluorene] significantly shifted the PL spectrum around 420 nm, which is deep blue region [19–21].

In this paper, we present the design and synthesis of spiro[fluorene-7,9′-benzofluorene]-based host and dopant materials substituted with naphthylanthraecenyl moiety at 2′-position and the investigation of their absorption and emission spectra, as well

* Corresponding author. Tel.: +82 41 5501476; fax: +82 41 5503431.
E-mail address: msgong@dankook.ac.kr (M.-S. Gong).

0143-7208/$ – see front matter © 2008 Elsevier Ltd. All rights reserved.
doi:10.1016/j.dyepig.2008.09.023

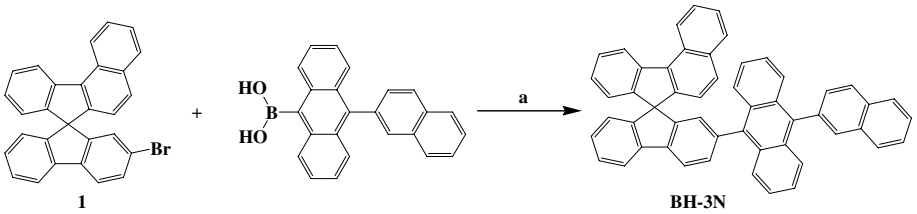

Scheme 1. (a) Tetrakis(triphenylphosphine)palladium(0), K_2CO_3, THF, 18 h, 80 °C, 73% yield.

as their electroluminescence properties as blue light-emitting materials.

2. Experimental

2.1. Material and measurements

2-Bromo-spiro[fluorene-7,9′-benzofluorene] (**1**) and 9-(2-naphthylanthracene)-10-boronic acid were synthesized according to the method previously reported [15]. Diphenyl-[4-(2-[1,1;4,1]terphenyl-4-yl-vinyl)-phenyl]-amine (BD-1), 2-[4′-(phenyl-4-vinylbenzene amine)phenyl-spiro[fluorene-7,9′-benzofluorene] (BH-3BD) and 4-[2-naphthyl-4′(phenyl-4-vinylbenzeneamine)]phenyl (BD-1N) were prepared by the method previously reported [20,21]. Tetrakis (triphenylphosphine)palladium(0) and potassium *t*-butoxide (Aldrich Chem. Co.) were used without further purification. Tetrahydrofuran (THF) was distilled over sodium and calcium hydride.

The ^{1}H NMR and ^{13}C NMR spectra were recorded on a Bruker, Avance 500 (500 MHz) spectrometer. The photoluminescence (PL) spectra were recorded on a fluorescence spectrophotometer (Jasco FP-6500) and the UV–vis spectra were obtained by means of an UV–vis spectrophotometer (Shimadzu, UV-1601PC). The energy levels were measured with a low-energy photo-electron spectrometer (Riken-Keiki AC-2). The FT-IR spectra were obtained with a Biorad Excaliber FTS-3000MX spectrophotometer and the elemental analyses were performed using a CE Instrument, EA1110. The DSC measurements were performed on a Mettler DSC 822^e under nitrogen at a heating rate of 10 °C/min. The low and high resolution mass spectra were recorded using a JEOL, JMS-AX505WA spectrometer in FAB mode.

2.2. Synthesis of 2-(10-naphthylanthracene)-spiro[fluorene-7, 9′-benzofluorene] (BH-3N)

A solution of **1** (5.0 g, 11.18 mmol), 9-(2-naphthylanthracene)-10-boronic acid (8.99 g, 13.41 mmol) and tetrakis(triphenylphos phine)palladium(0) (0.68 g, 0.59 mmol) dissolved in THF (100 mL) was stirred in a two-necked flask under a nitrogen atmosphere for 30 min. To the reaction mixture, potassium carbonate (1.63 g, 11.18 mmol) in distilled water (50 mL) was added dropwise over a period of 20 min. The resulting solution was refluxed overnight at 80 °C. The reaction mixture was extracted with dichloromethane and the organic layer was separated. After the organic layer was evaporated with a rotary evaporator, the resulting powdery product was purified by column chromatography using *n*-hexane as the eluent to give a white crystalline solid.

BH-3N: Yield 73%. Mp 332 °C. ^{1}H NMR (500 MHz, $CDCl_3$) δ 8.75–8.73 (d, 1H), 8.35–8.33 (d, 1H), 8.13–8.10 (d, 1H), 8.00–7.95 (m, 3H), 7.90–7.85 (d, 1H), 7.77 (s, 1H), 7.67–7.65 (m, 1H), 7.60–7.54 (m, 9H), 7.53–7.40 (m, 4H), 7.24–7.15 (m, 7H), 7.02–7.01 (d, 2H), 6.86 (s, 1H), 6.79–6.78 (d, 1H). ^{13}C NMR ($CDCl_3$) δ 149.6, 148.6, 143.1, 141.7, 130.1, 128.2, 128.1, 128.0, 127.5, 127.2, 126.9, 125.6, 125.2, 125.1, 124.4, 124.1, 123.2, 120.2, 120.2, 77.4, 77.2, 76.9, 66.5 ppm. FT-IR (KBr, cm^{-1}) 3059, 3040, 3012 (aromatic C-H). MS (FAB) *m*/*z* 668.0 [$(M+1)^+$]. Anal. Calcd. for $C_{55}H_{32}$ (442.55): C, 95.18; H, 4.82. Found: C, 94.66; H, 4.81. UV–vis (THF): λ_{max} (Absorption) = 369, 388 nm, λ_{max} (Emission) = 432 (THF), 447 nm (thin film).

2.3. OLED fabrication and measurement

Prior to the fabrication of the device, ITO with a resistance of 12 Ω/□ on glass was patterned as an active area of 4 mm^2. The substrates were cleaned by sonication in deionized water, boiled in IPA for 20 min, and dried with nitrogen. Finally, the substrates were dry cleaned using plasma treatment in an O_2 and Ar environment. Organic layers were deposited sequentially by thermal evaporation from resistively heated alumina crucibles onto the substrate at a rate of 1.0 Å/s. The thicknesses of the *N*,*N*′-bis[4-(di-*m*-tolylamino)phenyl]-*N*,*N*′-diphenylbiphenyl-4,4′-diamine (DNTPD, HIL), bis[*N*-(1-naphthyl)-*N*-phenyl]benzidine (α-NPD, HTL), Host:5% dopant (EML) and aluminum tris(8-hydroxyquinoline) (Alq_3, ETL) layers were about 400, 200, 300 and 200 Å, respectively. Before the deposition of the metal cathode, LiF was deposited onto the organic layers with a thickness of 10 Å. A high-purity aluminum cathode was deposited at a rate of 1–5 Å/s with a thickness of 2000 Å as the top layer.

After its fabrication and the venting of the evaporation with nitrogen gas, the device was immediately transferred to a glove box. A thin epoxy adhesive was applied from a syringe around the edge of a clean cover glass. To complete the package, a clean cover glass was placed on top of the device. The epoxy resin was cured under intense UV radiation for 3 min. The current–voltage characteristics of the encapsulated devices were measured on a programmable electrometer having current and voltage sources (Source Measure Unit, model Keithley 237). The luminance and EL spectra were measured with a PR650 system (Photo Research Co. Ltd.).

3. Results and discussion

3.1. Synthesis and characterization

2-(10-Naphthylanthracene)-spiro[fluorene-7,9′-benzofluorene] (BH-3N) was prepared through the Suzuki reaction of **1** with 9-(2-

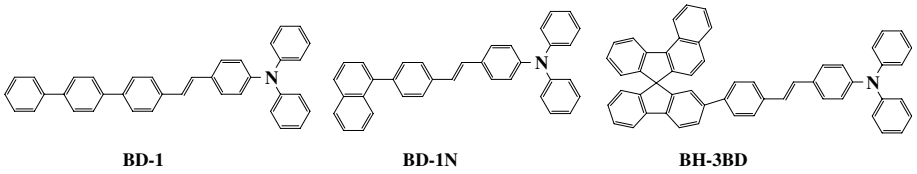

Scheme 2. Chemical structure of dopant materials, BD-1, BD-1N and BH-3BD.

naphthylanthracene)-10-boronic acid in the presence of a palladium catalyst in 73% yield as shown in Scheme 1. All the proton peaks were observed in the range of 6.78–8.75 ppm in the ^{1}H NMR spectra of BH-3N. The chiral carbon peak was observed at 66.50 ppm in the ^{13}C NMR spectrum of BH-3N. The results of the elemental analysis and mass spectroscopy also suggested the formation of BH-3N and matched well with the calculated data. The chemical structure of three dopant materials, diphenyl[4-(2-[1,1;4,1]terphenyl-4-yl-vinyl) phenyl]amine (BD-1), 2-[4′-(phenyl-4-vinylbenzeneamine)phenyl-spiro[fluorene-7,9′-benzofluorene] (BH-3BD) and 4-[2-naphthyl-4′(phenyl-4-vinylbenzeneamine)]phenyl (BD-1N) are illustrated in Scheme 2.

3.2. Thermal properties

The thermal properties of the spiro-based host and dopant materials, BH-3N, BH-3BD and BD-1N were investigated by differential scanning calorimetry (DSC) as shown in Table 1. In the first heating cycle, endothermic peaks were observed at 332 and 308.3 °C, due to the melting of BH-3N and BH-3BD, respectively. In the subsequent heating cycle, BH-3N and BH-3BD exhibited distinct glass transition temperatures of 226.1 and 195.2 °C, respectively, but did not undergo recrystallization or melting. The non-spiro dopant material BD-1N exhibits a distinct melting temperature of 204.8 °C, a glass transition temperature of 68.93 °C and a crystallization temperature of 97.7 °C. We attributed the thermal stability of the spiro-based host and dopant materials to the nonplanar and 3D-spiro-structure that arises from the incorporation of the spiro[fluorine-benzofluorene] moiety.

3.3. Optical properties

UV absorption and emission wavelengths are summarized in Table 2. Fig. 1a) shows the absorption spectrum of the BH-3N host material. The UV absorption spectrum of BH-3N exhibited two intense bands at 369 and 388 nm. The emission spectrum of the BH-3N thin film ($\lambda_{max} = 446$ nm) was prepared by spin-coating from a THF solution onto a quartz plate and was red-shifted by 14 nm comparing to that in dilute solution ($\lambda_{max} = 432$ nm). Fig. 1b depicts the absorption and PL spectra of the dopant materials BD-1 and BH-3BD in dilute solution and the thin solid films. The UV absorption spectra of the dopants are observable 369.5 nm for BD-1N and 375 nm for BH-3BD. The emission spectra of BD-1N and BH-3BD in THF show emission peaks at 452 and 469 nm, respectively. The emission spectrum of the solid thin film was red-shifted by 7.5 nm for BH-3BD and blue-shifted by 10 nm for BD-1N in comparison to its PL spectrum in dilute solution. The blue-shift of the emission observed in the solid thin film is probably due to the difference in relative permittivity or dielectric constant of the environment [22]. The solution fluorescence quantum efficiency (Φ_f) of host and dopant materials, all of which fall in the range of $\Phi_f = 0.67$–0.78, were determined relative to 9,10-diphenylanthracene in cyclohexane ($\Phi_f = 0.90$) [23]. The solution fluorescence quantum efficiency of host (95%) and dopant (5%) materials falls in the range of Φ_f 0.72–0.81. When we have measured PL spectra of doping system in film state, the wavelength of the PL spectra showed at 433 nm change and the intensities increased as doped with BD-1, BD-1N and BH-3BD.

Table 1
Thermal properties of new spiro-based host and dopant materials.

Temperature (°C)	Materials			
	BH-3N[d]	BD-1[e]	BD-1N[f]	BH-3BD[g]
T_g[a]	226.1	–	68.93	195.2
T_c[b]	–	–	97.7	–
T_m[c]	332	306.9	204.8	308.3

[a] Glass transition temperature.
[b] Crystallization temperature.
[c] Melting temperature.
[d] 2-(10-Biphenylanthracene)-spiro[fluorene-7,9′-benzofluorene].
[e] Diphenyl-[4-(2-[1,1;4,1]terphenyl-4-yl-vinyl)-phenyl]amine.
[f] 4-[2-Naphthyl-4′(phenyl-4-vinylbenzeneamine)]phenyl.
[g] 2-[4′-(Phenyl-4-vinylbenzeneamine)phenyl-spiro[fluorene-7,9′-benzofluorene].

Table 2
UV absorption and PL properties of BH-3N, BD-1, BD-1N and BH-3BD in THF solution and solid film.

Sample	UV absorption (nm)	PL (nm)		FWHM (nm)		Φ_f[a]
		Solution	Film	Solution	Film	
BH-3N	369, 388	432	447	54.0	59.1	0.67
BD-1	383	454	472	–	–	0.71
BD-1N	369.5	452	442	68.6	52.9	0.75
BH-3BD	375	469	476.5	70.9	52.4	0.78
BH-3N:5% BD-1	388.2	–	443.0	–	–	0.72
BH-3N:5% BD-1N	388.7	–	432.2	–	–	0.75
BH-3N:5% BH-3BD	388.5	–	433.0	–	–	0.81

[a] Fluorescence quantum efficiency, relative to 9,10-diphenylanthracene in cyclohexane ($\Phi_f = 0.90$).

3.4. The estimation of HOMO and LUMO energy levels

A low-energy photo-electron spectrometer was used to obtain information about the HOMO and LUMO energy values of the host

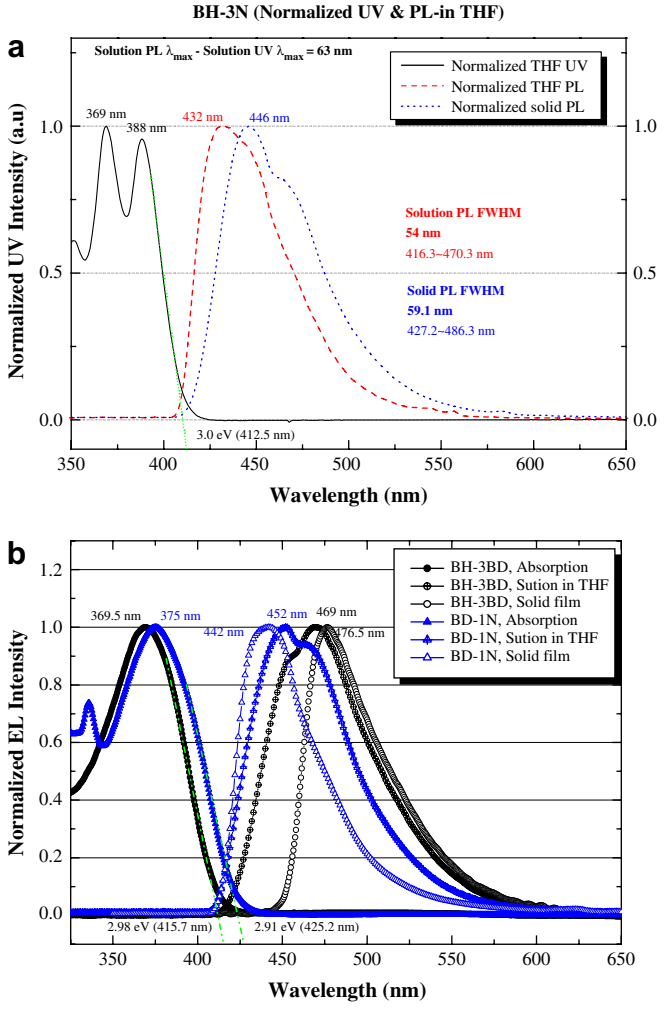

Fig. 1. Normalized absorption and photoluminescence spectra of (a) BH-3N host and (b) BD-1N and BH-3BD dopant materials.

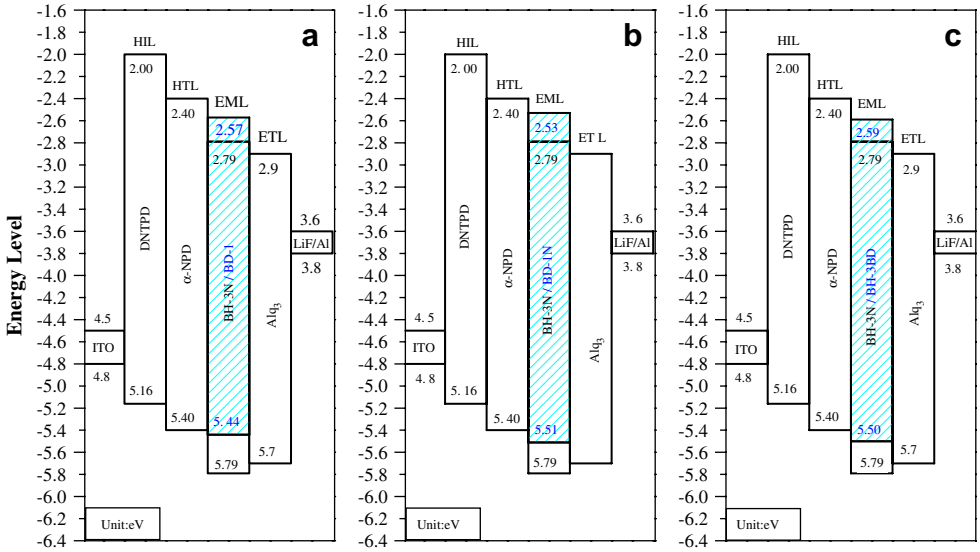

Fig. 2. Energy diagram of BH-3N doped with (a) BD-1, (b) BD-1N and (c) BH-3BD.

and dopant materials and to examine the barriers for charge injection. The HOMO energy level of BH-3N was determined to be 5.79 eV. The LUMO energy level of BH-3N was estimated to be 2.79 eV. BH-3N showed an UV–vis absorption maximum at 388 nm and its onset at 412.5 nm corresponding to a band gap of 3.00 eV. Fig. 2 summarizes the HOMO and LUMO energies of the four compounds. The energy gaps of the dopant materials BD-1N and BH-3BD were 2.98 and 2.91 eV, respectively, and are located in the region of blue light emission.

3.5. Performance in OLEDs

In this study, an EL device was fabricated using DNTPD as the hole injection layer, α-NPD as the hole transport layer, Alq_3 as the electron transport layer, BH-3N host:5% dopant as the emitting layer, ITO as the anode, LiF as the buffer layer, and Al as the cathode. These formed a structure consisting of ITO/DNTPD/NPB/BH-3N:5% dopant/Alq_3/Al-LiF.

The EL spectra of device 1 without the dopant and device 3 (doped with BD-1N) both appeared at 448 nm. The EL spectra of devices 1 and 3 correlate very well with the PL spectrum of BH-3N. The EL spectrum of device 3 using the BD-1N dopant is almost identical to the PL spectrum of BD-1N. This suggests that energy is efficiently transferred from the BH-3N host to the BD-1N dopant. On the other hand, the EL spectra of device 2 (doped with BD-1) and 4 (doped with BH-3BD) were red-shifted by 4–8 nm to longer wavelengths than their PL spectra, as shown in Fig. 3. The CIE coordinates of devices 2, 3 and 4 using Alq_3 as an ETL material are $x = 0.15$, $y = 0.14$, $x = 0.16$, $y = 0.14$ and $x = 0.15$, $y = 0.14$, respectively. The CIE coordinates of device 4 without a dopant are $x = 0.15$ and $y = 0.11$, which is a deep blue color.

The primary OLED measurement is the luminance–voltage (L–V) curve. One applies a fixed voltage to a device and then measures the resulting light output. The luminance–voltage curves clearly show that the devices have a low turn-on voltage of 4.5 V, as shown in Fig. 4. Device 3 showed a luminance of 665.7 cd/m^2 at a current density of 17.93 mA/cm^2 at 7 V, which is twice the value of device 1 without a dopant. Device 4 (ITO/DNTPD/NPB/BH-3N:5% BH-3BD/Alq_3/Al-LiF) exhibited an EL spectrum of 456 nm and its maximum luminance was increased to 5018 cd/m^2 at 10 V as compared to 2476 cd/m^2 for device 1 without a dopant. In the case of device 2,

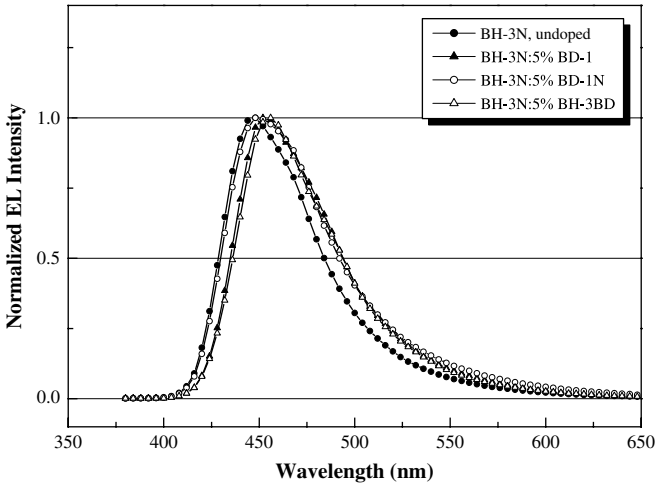

Fig. 3. EL spectra of the devices obtained from BH-3N host doped with various dopants.

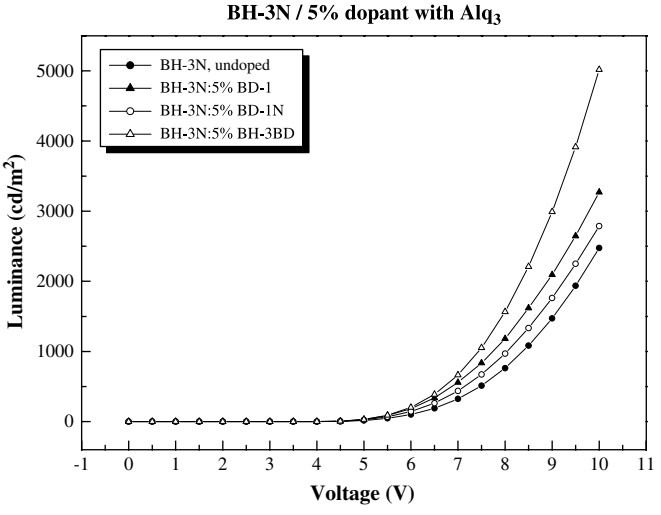

Fig. 4. Luminance–voltage curves for the ITO/DNTPD/NPB/BH-3N:5% dopant/Alq_3/Al–LiF devices.

Table 3
EL properties of the devices obtained from new spiro-type host and dopant materials.

Properties		Devices			
		1	2	3	4
EL at 7 V	λ_{max} (nm)	448	452	448	456
	mA/cm^2	15.25	17.18	18.77	17.93
	cd/A[a]	2.12	3.25	2.32	3.71
	lm/W[b]	0.95	1.46	1.04	1.66
	cd/m^2	323.7	559.4	437.5	665.7
	CIE-x	0.15	0.15	0.16	0.15
	CIE-y	0.11	0.14	0.14	0.14

1, BH-3N, undoped; 2, BH-3N:5% BD-1; 3, BH-3N:5% BD-1N, 4, BH-3N:5% BH-3BD.
[a] Luminous efficiency is defined as the ratio of luminous flux to total radiated flux. Luminous efficiency is the ratio of the luminance (cd/m^2) to the current density (A/m^2), and has unit of cd/A.
[b] The power efficiency is the ratio of the light output in lumen divided by the electrical input Watts.

a luminance of 559.4 cd/m^2 was observed at 17.18 mA/cm^2, which was comparable to the value of 323.7 cd/m^2 at 15.25 mA/cm^2 of device 1 without a dopant (Table 3). The results suggest that the use of BH-3N shows promise as a blue-emitting layer material. Fig. 5 shows the dependence of the current density on the voltage for devices obtained from BH-3N doped with BD-1, BD-1N and BH-3BD.

The current is converted to current density to account for the lateral area of the OLED. Fig. 6 shows current efficiencies as a function of the current density for devices 1–4. Luminous efficiency is defined as the ratio of luminous flux to total radiated flux. Luminous efficiency is the ratio of the luminance (cd/m^2) to the current density (A/m^2), and has unit of cd/A. It was clearly shown that the luminance efficiency of device 4 was higher than that of devices 1, 2 and 3. As the current density increased, the current efficiency of device 4 increased abruptly to 3.71 cd/A at 17.93 mA/cm^2. This phenomenon is caused by the formation of the excitons required to emit light. The most important observation in this figure is that the efficiency of the devices remains quite stable when the current density is changed from 20 to 150 mA/cm^2. The efficiency at 150 mA/cm^2 only decreased by about 10% as compared with that at 20 mA/cm^2.

Device 2 showing a deep blue EL spectrum of 452 nm exhibited an efficiency of 3.25 cd/A. Device 4, consisting of ITO/DNTPD/NPB/BH-3 N:5% BH-3BD/Alq_3/Al-LiF, exhibited a relatively higher efficiency of 3.71 cd/A at 7 V in its current efficiency–voltage relation, as shown in Fig. 7. Band gap, HOMO and LUMO of BD-1, BH-3BD and BD-1N were similar and only the molecular structure of dopant materials was different. However, among the three dopant materials, the efficiency of device doped with BH-3BD was higher than those of BD-1 and BD-1N. It was reported that the emitting layer with smaller asperities resulted in enhanced device performance [10]. A thin layer of BH-3P:5% BH-3BD displays a fairly good surface morphology. It is apparent that the presence of the spiro[fluorine-7,9′-benzofluorene] core inhibits the crystallization of BH-3BD, with the effect of maintaining its morphological stability in a glassy state. The surface roughness of BH-3N:BH3BD and BH-3N:BD-1 surface was investigated by the tapping mode atomic force microscopy. The root mean square (RMS) surface roughness of BH-3N:BH-3BD was *ca.* 1.53 nm, whereas the surface roughness of BH-3N:BD-1 was *ca.* 6.77 nm. Compared to the BH-3N:BD-1, BH-3N:BH-3BD layer provided the better surface contact at ETL interface. Based on these results, it was found that the spiro-type host and dopant materials were very effective in improving the EL efficiency in the structure of the BH-3N:5% BH-3BD/Alq_3 device.

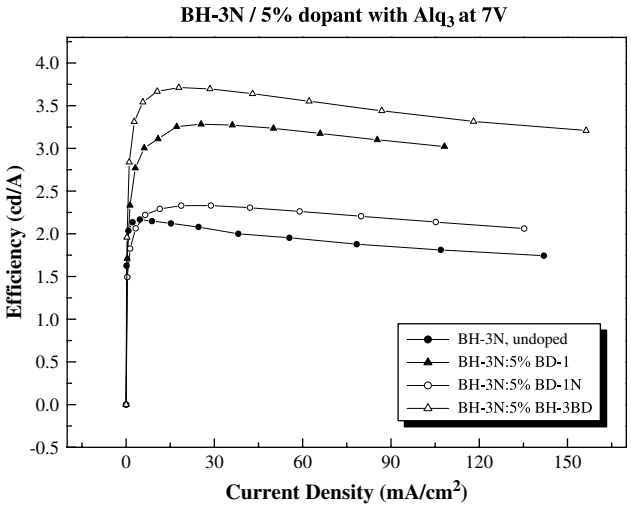

Fig. 6. Efficiency–current density characteristics of the ITO/DNTPD/NPB/BH-3N:5% dopant/Alq_3/Al–LiF devices.

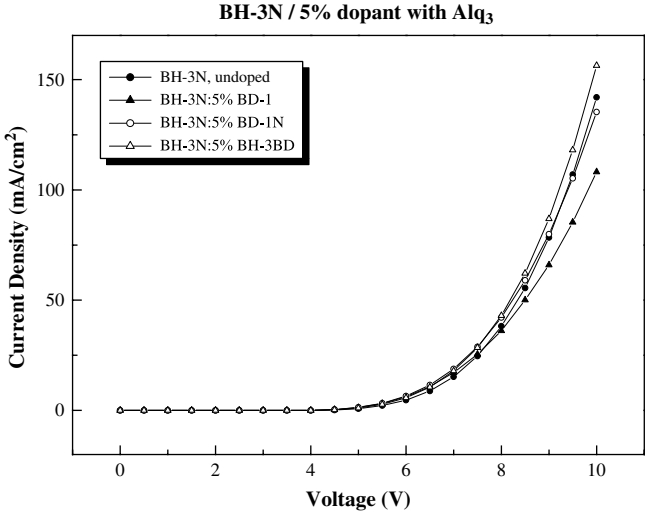

Fig. 5. Current density–voltage characteristics of the ITO/DNTPD/NPB/BH-3N:5% dopant/Alq_3/Al-LiF devices.

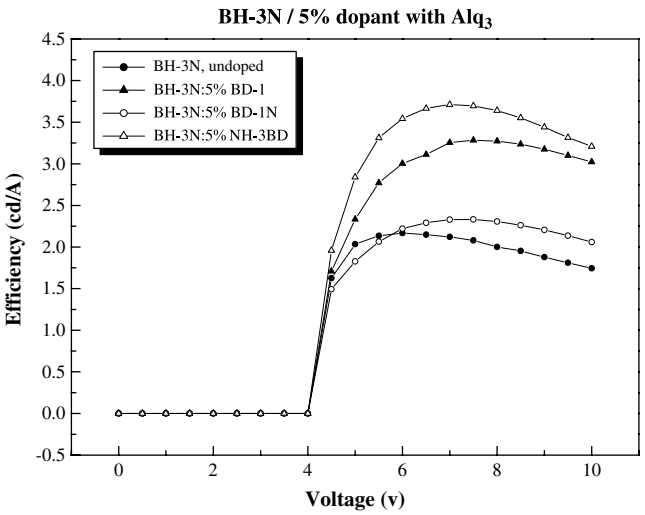

Fig. 7. Efficiency–voltage characteristics of the ITO/DNTPD/NPB/BH-3N:5% dopant/Alq_3/Al–LiF devices.

4. Conclusions

New blue host material based on spiro[fluorine-benzofluorene] derivative was successfully prepared and used to construct blue OLEDs. The EL emission spectra of the devices are between 448 and 456 nm. The CIE coordinates of the device made of BH-3N:5% BH-3BD were $x = 0.15$ and $y = 0.14$, and these are good color coordinate values for blue emission. The device fabricated using the BH-3BD dopant has a maximum luminance of 5018 cd/m^2 at a current density of 156.36 mA/cm^2, and its maximum power efficiency is 3.20 cd/A. The measurement tests of the lifetime of the devices and the examination of the EL characteristics of devices using other commercially available dopants are now in progress. These results will be presented elsewhere in the near future.

Acknowledgement

This work was supported by grant No. RT104-01-02 from the Regional Technology Innovation program of the Ministry of Knowledge Economy (MKE).

References

[1] Tang CW, Slyke Van. Organic electroluminescent diodes. Appl Phys Lett 1987;51:913–5.
[2] Kim KS, Jeon YM, Kim JW, Lee CW, Gong MS. Blue organic light-emitting devices using novel styrylarylene host and dopant materials. Dyes Pigments 2008;78:238–44.
[3] Seong NC, Jeon YM, Lim TH, Kim JW, Lee CW, Lee EJ, et al. Organic light-emitting device using new distyrylarylene host materials. Synth Met 2007;257:421–6.
[4] Lee MT, Liao CH, Tsai CH, Chen CH. Highly Efficient, deep-blue doped organic light-emitting devices. Adv Mater 2005;17:2493–7.
[5] Ho MH, Wu YS, Wen SW, Lee MT, Chen TM, Chen CH, et al. Highly efficient deep blue organic electroluminescent device based on 1-methyl-9,10-di(1-naphthyl)anthracene. Appl Phys Lett 2006;89:252903–5.
[6] Gao ZQ, Mi BX, Chen CH, Cheah KW, Cheng YK, Wen WS. High-efficiency deep blue host for organic light-emitting devices. Appl Phys Lett 2007;90:123506–8.
[7] Wu R, Schumm JS, Pearson DL, Tour JM. Convergent synthetic routes to orthogonally fused conjugated oligomers directed toward molecular scale electronic device applications. J Org Chem 1996;61:6906–21.
[8] Xiao H, Leng B, Tian H. Hole transport triphenylamine–spirosilabifluorene alternating copolymer: synthesis and optical, electrochemical and electroluminescent properties. Polymer 2005;46:5707–13.
[9] Xiao H, Shen H, Lin Y, Su J, He Tian. Spirosilabifluorene linked bistriphenylamine: synthesis and application in hole transporting and two-photon fluorescent imaging. Dyes Pigments 2007;73:224–9.
[10] Salbeck J, Yu N, Bauer J, Weissortel F, Bestgen H. Low molecular organic glasses for blue electroluminescence. Synth Met 1997;91:209–15.
[11] Katsis D, Geng YH, Ou JJ, Culligan SW, Trajkovska A, Chen SH, et al. Spiro-linked ter-, penta-, and heptafluorenes as novel amorphous materials for blue light emission. Chem Mater 2002;14:1332–9.
[12] Bach U, Cloedt KD, Spreitzer H, Gratzel M. Characterization of hole transport in a new class of spiro-linked oligotriphenylamine compounds. Adv Mater 2000;12:1060–3.
[13] Mitschke U, Bäuerle P. Synthesis, characterization, and electrogenerated chemiluminescence of phenyl-substituted, phenyl-annulated, and spirofluorenyl-bridged oligothiophenes. J Chem Soc Perkin Trans 1 2001;8:740–53.
[14] Saragi TPI, Spehr T, Siebert A, Fuhrmann-Lieker T, Salbeck J. Spiro compounds for organic optoelectronics. Chem Rev 2007;107:1011–65.
[15] Prelog V, Bedekovic D. Chirale 2,2′-polyoxaalkano-9,9′-spirobifluorene. Helv Chim Acta 1979;62:2285–302.
[16] Harada N, Ono H, Nishiwaki T, Uda H. Synthesis, circular dichroism and absolute stereochemistry of chiral spiroaromatic compounds. 9,9′-Spirobifluorene derivatives. J Chem Soc Chem Commun 1991:1753–5.
[17] Alcazar V, Diederich F. Enantioselektive komplexierung chiraler dicarbonsäuren in funktionalisierten spaltenförmigen 9,9′-spirobifluorenen. Angew Chem 1992;104:1503–5.
[18] Cuntze J, Diederich F. Molecular recognition and enantiomer separations on a novel chiral stationary phase based on a 9,9′-spirobi[9H-fluorene]-derived molecular cleft. Helv Chim Acta 1997;80:897–911.
[19] Jeon SO, Jeon YM, Kim JW, Lee CW, Gong MS. Blue organic light-emitting diode with improved color purity using 5-naphthyl-spiro[fluorene-7,9′-benzofluorene]. Org Electron 2008;9:522–9.
[20] Kim KS, Jeon YM, Kim JW, Lee CW, Gong MS. Blue light-emitting OLED using new spiro[fluorene-7, 9′-benzofluorene] host and dopant materials. Org Electron 2008;9:797–804.
[21] Kim KS, Jeon YM, Kim JW, Lee CW, Gong MS. Blue organic electroluminescent devices based on the spiro[fluorene-7,9′-benzofluorene] derivatives as host and dopant materials. Synth Met; in press.
[22] Chen SF, Wang CW. Influence of the hole injection layer on the luminescent performance of organic light-emitting diodes. Appl Phys Lett 2004;85:765–9.
[23] Hamai S, Hirayama F. Actinometric determination of absolute fluorescence quantum yields. J Phys Chem 1983;87:83–9.